Impact of nanometric processes linked to charge generation on the macroscopic behaviour in polyethylene

Q.M. Hoang, Séverine Le Roy

Impact of nanometric processes linked to charge generation on the macroscopic behaviour in polyethylene

Q.M. Hoang[1] and S. Le Roy[2]
[1]Faculty of Electrical Engineering, Hanoi University of Industry, Hanoi, Vietnam,
[2] LAPLACE, Université de Toulouse, CNRS, INPT, UPS, Toulouse, France

***Abstract*- Electric field distribution in polymer electrical insulations under DC constraints is directly linked to the presence of charges within the material. Space charge generation is thought to mainly arise from injection at the electrodes, in polyethylene based materials. Hence, describing this injection is still a challenge. Surface roughness, increase of the energy levels linked to the physical interface, variation of these energy levels along the surface are among the physical hypotheses that impact the charge injection, and these hypotheses take place at the nanometric or micrometric scale. A bipolar charge transport model, developed in 2D, is presented, and accounts for these different physical hypotheses at the electrode in order to observe the impact of each process on the space charge behavior at the macroscopic scale.**

I. INTRODUCTION

Predicting the electric field distribution in polymers used as electrical insulators remains of prime importance for DC applications. Charges, generated at the electrodes or inside the bulk, disturb the electric field distribution, leading to local field enhancements, and potentially to an early breakdown. Bipolar charge transport models, also called BCT or mesoscopic models [1-3], have been developed this last two decades to predict the electric field distribution within such insulating materials. Electronic charges generation (electrons or holes) at the electrodes are generally described as charge injection, either using the thermionic –i.e. Schottky, or a tunneling, i.e. Fowler Nordheim equation. These physical hypotheses are however too simple, and do not account for the particular material structure of the material at an interface, directly related to barrier injection, and/or energy states, and lastly to surface roughness. Experimental [1-2] and theoretical researches [3-5] have focused on this particular interface behaviour, but a lot remains to do. In the present paper, we propose a 2D charge transport model developed to account for different physical processes related to the interface: surface roughness, variation of the injection barrier height along the x axis related to a variation of the material structure, and an interfacial zone of 1 µm where the energy states are deeper and with a higher density. Simulated results for each case study show that each physical hypothesis leads to a different impact on the space charge behaviour.

II. MODEL DESCRIPTION

A bipolar charge transport model, already published in the literature [5], has been developed in two dimensions with a commercial finite element modelling (FEM) software. The sample considered is a low density polyethylene (LDPE) of thickness 150 µm, and a width of 45 µm. It is considered as homogeneous in the third dimension. An electric field of 40 kV/mm is applied on the sample at T=25°C, which corresponds to an applied voltage of 6 kV. The top electrode is considered as the anode, while the bottom electrode is grounded. The model accounts for electronic species (electrons and holes), generated by injection at each electrode, depending on the sign of the applied electric field, transport using a constant effective mobility which already takes into account the possible trapping and detrapping into shallow traps, trapping into a single level of deep traps for each kind of carriers, from which charges can detrap using a thermally activated coefficient, and recombination of charges of opposite sign, with constant parameters. A schematic representation of the model hypotheses is proposed on Fig. 1. The equations to solve are of the form:

$$\frac{\partial n_a}{\partial t} + \nabla.\left(\pm n_a \mu_a E - D_a \nabla n_a\right) = s_a \qquad (1)$$

$$\nabla.\left(\varepsilon_0 \varepsilon_r E\right) = \rho \qquad (2)$$

Where n_a is the charge density (C/m^3), a refers to the charge carrier, i.e. electron (e) or hole (h), mobile (µ) or trapped (t). t is the time, μ_a the mobility (m^2/V/s), for each carrier. E is the electric field (V/m), ε_0 the vacuum permittivity, ε_r the relative permittivity of the material and ρ the net charge density (C/m^3). All variables in equations (1-2) and in the following equations are space and time dependent, even if they are not

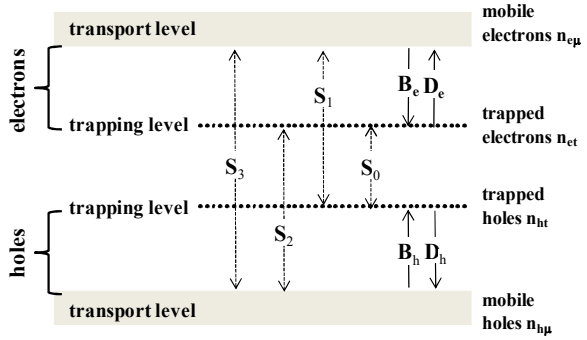

Fig. 1. Schematic representation of the two-levels of traps transport model. Conduction is by free charges in the transport levels, associated with a constant mobility.

presented so, for sake of simplicity. D_a refers to the diffusion coefficient, and follows the Einstein relation of the form:

$$D_a = \frac{k_B T}{e}\mu_a \quad (3)$$

k_B is the Boltzmann's constant, e the elementary charge and T the temperature (K). s_a are the source terms, reflecting all the physical processes not linked to transport, and are detailed in [6].

Charge generation is only due to injection of carriers at each electrode, and follows the Schottky law:

$$j_{Schott}(A-C)) = AT^2 \exp\left(\frac{-ew_{ai}}{k_B T}\right)\exp\left(\frac{e}{k_B T}\sqrt{\frac{eE_{A-C}}{4\pi\varepsilon_0\varepsilon_r}}\right) \quad (4)$$

A is the Richardson's constant, w_{ai} is the injection barrier height, for electrons or holes (eV), and the coordinate A or C refers to the anode or to the cathode respectively. No extraction barriers are accounted for at the electrodes, so the extraction fluxes for holes at the cathode and for electrons at the anode are of the form:

$$j_{a,ext} = \pm n_a \mu_a E - D_a \nabla n_a \quad (5)$$

The model has been applied to a polyethylene based material, for which optimized parameters have been published in the literature for a one-dimension model [6], and are listed in Table I. The present model, developed with COMSOL Multiphysics® uses the Transport of Diluted Species (TDS) module to solve the continuity equation for each kind of carrier [5]. This module already includes stabilization solutions to prevent oscillations. The Poisson equation module is used to couple these equations to the Poisson's equation. Backward Differentiation Formula solver is used for the time integration (maximum order 2, and minimum order 1). A zero flux is set as boundary conditions on the left and right sides. Before voltage application, the material is free of charges.

III. Simulation Results

All simulations in the present paragraph have been performed for an applied voltage of 6 kV. The voltage is applied for 2400s.

TABLE I. Parameters used for the simulations

Symbol	value	units
Trapping coefficients		
B_e electrons	1. 10^{-1}	s^{-1}
B_h holes	2. 10^{-1}	s^{-1}
Mobility for x and z axis		
μ_e for electrons	1. 10^{-14}	$m^2/V/s$
μ_h for holes	2. 10^{-13}	$m^2/V/s$
Trap densities		
N_{oet} for electrons	100	$C.m^{-3}$
N_{oht} for holes	100	$C.m^{-3}$
Injection barrier heights		
w_{ei} for electrons	1.27	eV
w_{hi} for holes	1.16	eV
Recombination coefficients		
S_0, S_1 and S_2	4. 10^{-3}	$m^3/C/s$
S_3	0	$m^3/C/s$
Relative permittivity	2.3	
Detrapping barrier heights		
w_{tre} for electrons	0.96	eV
w_{trh} for holes	0.99	eV

It allows observing specific behavior short time after voltage application, while keeping the simulation time relatively low. All simulations results are presented to be comparable to experimental data, i.e. the net charge density calculated in 2D is integrated over the x axis, and plotted as a function of depth and time [5], as what is proposed for space charge measurements. Influence charges are not added to the surface plot, in order to clearly observe the differences between the different cases study. These data are compared to simulated results where no hypothesis is accounted for, i.e. only a constant barrier height is taken into account for the Schottky injection (Fig. 2). The net charge density as a function of the y axis for a time of 300s is presented on Fig. 3 (black line), to better observe the impact of the interface hypotheses on the net charge density results at relatively short times.

A. *Surface roughness*

Simulations have been performed in the presence of a surface roughness at the anode only. Previous studies [3,5] have shown that concave defects increase the local electric field to a larger extent. To account as simply as possible for surface roughness, protusions having an elliptic shape have been simulated on a length of 10µm at the anode. The longest defect is 800 nm, the smallest one is 200 nm. The width of the ellipses varies between 50 nm and 400 nm. Fig. 4a presents the simulated surface

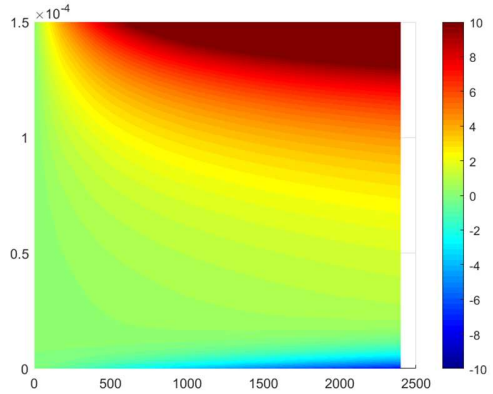

Fig. 2. Net charge density cartography as a function of time and depth in the sample (y) when only Schottky injection is considered. Horizontal axis: time in s. The colour scale provides charge density in C/m^3.

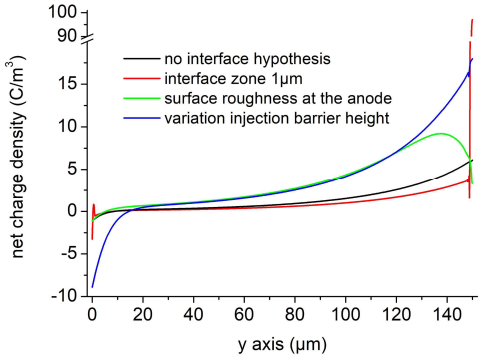

Fig. 3. Net charge density for different hypotheses on the charge generation at interfaces, compared to the case where no hypothesis is accounted for, and for t=300s. Parameters of Table I, unless otherwise stated.

roughness at the anode, while Fig. 4b presents the net charge density simulated results for this case study. It is to note that for this case study, the meshing needs to be adapted to such small size (i.e. some nanometers), while the sample thickness is 150µm. This is why only a rough anode is simulated. The net charge density as a function of the y axis for a time of 300s for this case study is also proposed in Fig. 3 (green line). The overall space charge density behavior is comparable to the one observed when no specific hypothesis is accounted for at the interfaces, i.e. a large injection of positive charges at the anode at short time. However, the injected positive charge density penetrates faster and with a higher density inside the bulk when the electrode is rough. The positive charge density is so high that it decreases the electric field at the anode, preventing more positive charges to be injected. This is clearly visible on Fig. 3, where the net charge density near the anode decreases. As the roughness represents only ¼ of the total electrode, the impact of roughness on the space charge behavior is non negligible.

B. Variation of the barrier height along the x axis

A way to account for the variation of the interface chemical structure is to set a variable injection barrier height along each electrode (x axis). This could account for the variation of energy states along the electrode, due to chain conformation, available energy levels for injection, variation of the barrier to injection from the Fermi level of the electrode to the energy state where charge is injected, etc. The injection barrier height for electrons and holes has then been calculated as being a random value along the x axis. A minimal and maximal value have been set for each barrier height, and are calculated as being ±10% of the 'optimized barrier height' (i.e. parameters of Table 1). This percentage has been chosen arbitrarily, and could be in reality larger. An example of barrier height distribution calculated for electrons at the cathode is proposed on Fig. 5. The number of points for this distribution is set to 25, and it is then extrapolated along the x axis. These barrier height values are then inserted in the fluid model, and calculations are performed for an applied voltage of 6 kV during 2400s. Fig. 6 presents the simulated net charge density as a function of time and space for this case study. The net charge density as a function of the y axis for a time of 300s is proposed in Fig. 3 (blue line). The charge behaviour for this case study compared to a homogeneous injection barrier height is almost the same, i.e. a large injection of positive charges at the anode, while negative charges injection is lower. However, the dynamic seems faster in the present case compared to the one with no barrier height variation (Fig. 3). Positive charges penetrate faster and with a higher amount within the bulk material. The same conclusion also holds for negative charge injection at the cathode, that are easily observable in the present case, while only a small amount of negative charges is injected in Fig. 3. The charge behavior is somehow different from the case where a rough electrode is simulated. In the case of a variation of the barrier height along the x axis, the injection of charges does not seem to be limited as in the case of a rough electrode (see the decrease of positive charge at the vicinity of the anode on Fig. 3). In the case of a variation of the barrier height, charge injection is enhanced when the barrier height is relatively small, while charge injection is lowered when the barrier height is

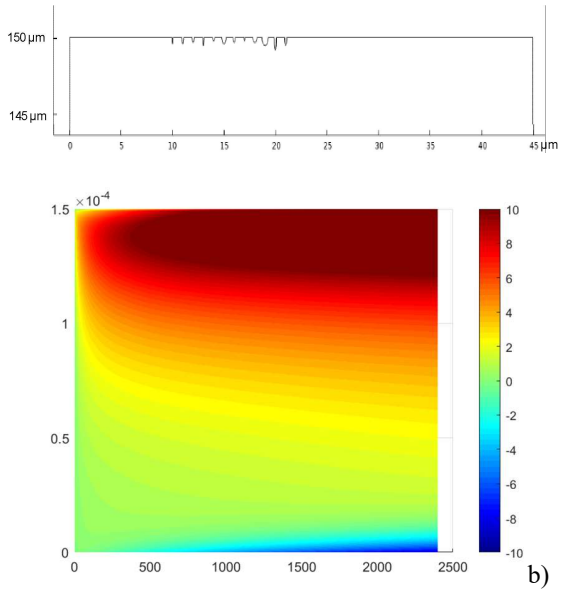

Fig. 4. a) Zoom of the rough zone on the top electrode surface, and b) Net charge density cartography as a function of time and depth in the sample, for a rough top electrode as proposed in Fig. 4a.

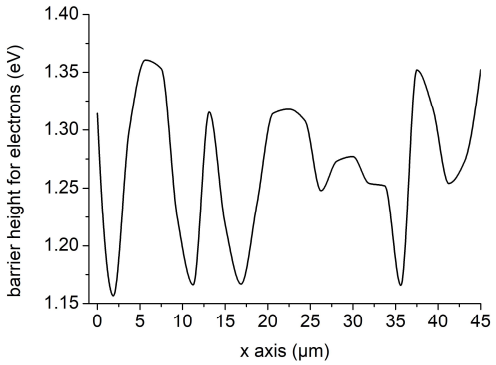

Fig. 5. Example of barrier height distribution as a function of x axis for electrons. The distribution is calculated as being in the range ±10% of the optimized value presented in Table 1.

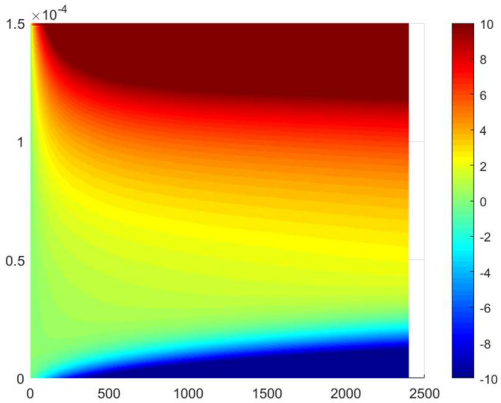

Fig. 6. Net charge density cartography as a function of time and depth in the sample, for a variation of the barrier height for electrons and holes of 10% around the optimized value found in Table 1.

high. The overall integrated behaviour leads to a case where the charge injection is fastened, as observed in Fig. 5, but the electric field is not decreased enough to have a limitation of the charge injection. It is to note that a large number of simulations have been performed with random barrier height distributions for electrons and holes, and the space charge behavior remains the same for each simulation.

C. Presence of an interfacial zone of 1 µm

An interfacial zone can also be present at each electrode, where the density of energy states is higher than in the bulk, with deeper traps. This kind of hypothesis has already been used in a BCT model using an exponential distribution of traps [7]. In the present case, we kept a two level of traps BCT model, with parameters for trapping, detrapping, and the number of available traps being higher compared to the ones of Table 1, for an interfacial zone of 1µm at each electrode for electrons and for holes. The way these parameters vary is chosen arbitrarily as linear, although any kind of variation could be proposed, as it is difficult in reality to have access to such information. The maximal trap density is set to 1000 C/m^3 for holes and 500 C/m^3 for electrons, the trapping coefficient decreases linearly from 20 to 0.2 s^{-1} for holes and from 1 to 0.1 s^{-1} for electrons, the detrapping barrier height decreases from 1.02 to 0.99 eV for holes and from 1 to 0.96 eV for electrons. Here also, the parameters chosen for the interface zone have been set arbitrarily, to enhance holes trapping compared to electrons. We do not discuss here the reality of the parameters, but only want to see the impact of this interface zone on the overall space charge behaviour, for the present model. Fig. 7 presents the simulated net charge density as a function of time and space for this case study. The net charge density as a function of the y axis for 300s is proposed on Fig. 3 (red line). The global space charge behaviour is comparable to the one when no interface zone is considered. Short time after voltage application, positive charges are visible in a large amount next to the anode. The presence of a higher amount of positive charges trapped at the anode (Fig. 3) seems to decrease hole injection, which is lower than the one with only a Schottky injection. At the cathode, electron injection seems not really impacted by an interface zone. Holes trapping is also enhanced at this interface zone. These heterocharges could locally enhance the electric field, leading to an enhanced negative charge injection. This is however not the case. A second point is that the presence of positive charges in this area needs to be counterbalanced before any net negative charges can be observed. Other parameters have been tested with almost the same results, i.e. no real change in the space charge pattern. This is however not what has been observed in [6]. The fact that the mobility is not field dependent might be of prime importance and will need to be tested in the future simulations. This interface zone could however change to a large extent other variables such as the current density or the recombination rate, which has been related to luminescence measurements.

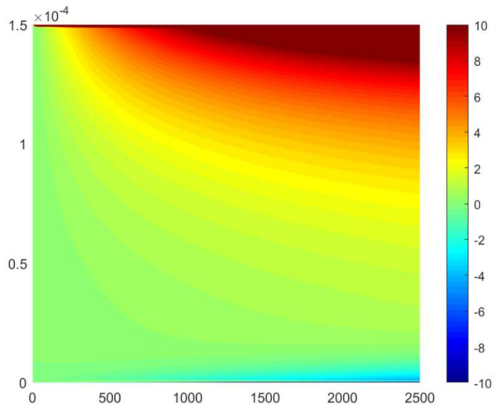

Fig. 7. Net charge density cartography as a function of time and depth in the sample, for an interface zone of 1µm at each electrode. Parameters in the bulk are those of Table 1.

IV. Conclusions

A bipolar charge transport model is proposed with specific hypotheses as regards the electrode/insulation interface. Rough electrodes and variation of the barrier height along the x axis lead almost to the same kind of space charge behavior, i.e. an increase of the net injected charge at each short time after voltage application, as well as a fastening of the injection process due either to a lower injection barrier height or to a local increase of the electric field due to protusions. The electric field is however not decreased enough in the case of a variation of the barrier height to decrease the positive charge injection. On the contrary, the addition of an interfacial zone leads to a different kind of net charge density, the most important point being the formation of heterocharges at each electrode.

Acknowledgment

This research is partly funded by Vietnam National Foundation for Science and Technology Development (NAFOSTED) under grant number 103.02-2019.33.

References

[1] E. Doedens , E.M. Jarvid, R. Guffond and Y.V. Serdyuk, “Space Charge Accumulation at Material Interfaces in HVDC Cable Insulation Part I—Experimental Study and Charge Injection Hypothesis “, *Energies*, vol. 13, 2005 (16p), 2020.

[2] M. Taleb, G. Teyssedre and S. Le Roy, “Role of the Interface on Charge Build-up in a Low-Density Polyethylene: Surface Roughness and Nature of the Electrode” *Proc. IEEE Conf. on Electrical Insulation and Dielectric Phenomena*, pp. 112-115, 2009.

[3] E. Doedens , E.M. Jarvid, R. Guffond and Y.V. Serdyuk, “Space Charge Accumulation at Material Interfaces in HVDC Cable Insulation Part II—Simulations of Charge Transport “, *Energies*, vol. 13, 1750 (24p), 2020.

[4] M. El-Shahat, A. Huzayyin and H. Anis, "Effect of morphological deformation on barriers to charge injection at the interface of copper and polyethylene", *IEEE Trans. Dielectr. Electr. Insul.*, vol. 25, pp. 2178-82, 2018.

[5] M.Q. Hoang, M.Q. Nguyen, T.T.N. Vu, G. Teyssedre and S. Le Roy, “Modelling the impact of electrode roughness on net charge density in polyethylene”, *J. Phys. D : Appl. Phys.*, vol. 54, 305303 (7p), 2021.

[6] S. Le Roy S, G. Teyssedre, C. Laurent, G.C. Montanari and F. Palmieri, “escription of charge transport in polyethylene using a fluid model with a constant mobility: fitting model and experiments”, J. Phys. D: Appl. Phys., vol. 39, pp. 1427-36, 2006.

[7] M. Taleb, G. Teyssèdre, S. Le Roy and C. Laurent, “Modeling of Charge Injection and Extraction in a Metal/Polymer Interface through an Exponential Distribution of Surface States”, IEEE Trans. Dielectr. Electr. Insul., vol. 20, pp. 311-20, 2013.